JACS
JOURNAL OF THE AMERICAN CHEMICAL SOCIETY
pubs.acs.org/JACS
Article

Metal–Organic Bichromophore Lowers the Upconversion Excitation Power Threshold and Promotes UV Photoreactions

Han Li, Cui Wang, Felix Glaser, Narayan Sinha, and Oliver S. Wenger*

Cite This: J. Am. Chem. Soc. 2023, 145, 11402–11414
Read Online
ACCESS | Metrics & More | Article Recommendations | Supporting Information

ABSTRACT: Sensitized triplet–triplet annihilation upconversion is a promising strategy to use visible light for chemical reactions requiring the energy input of UV photons. This strategy avoids unsafe ultraviolet light sources and can mitigate photo-damage and provide access to reactions, for which filter effects hamper direct UV excitation. Here, we report a new approach to make blue-to-UV upconversion more amenable to photochemical applications. The tethering of a naphthalene unit to a cyclometalated iridium(III) complex yields a bichromophore with a high triplet energy (2.68 eV) and a naphthalene-based triplet reservoir featuring a lifetime of 72.1 μs, roughly a factor of 20 longer than the photoactive excited state of the parent iridium(III) complex. In combination with three different annihilators, consistently lower thresholds for the blue-to-UV upconversion to crossover from a quadratic into a linear excitation power dependence regime were observed with the bichromophore compared to the parent iridium(III) complex. The upconversion system composed of the bichromophore and the 2,5-diphenyloxazole annihilator is sufficiently robust under long-term blue irradiation to continuously provide a high-energy singlet-excited state that can drive chemical reactions normally requiring UV light. Both photoredox and energy transfer catalyses were feasible using this concept, including the reductive N–O bond cleavage of Weinreb amides, a C–C coupling reaction based on reductive aryl debromination, and two Paternò–Büchi [2 + 2] cycloaddition reactions. Our work seems relevant in the context of developing new strategies for driving energetically demanding photochemistry with low-energy input light.

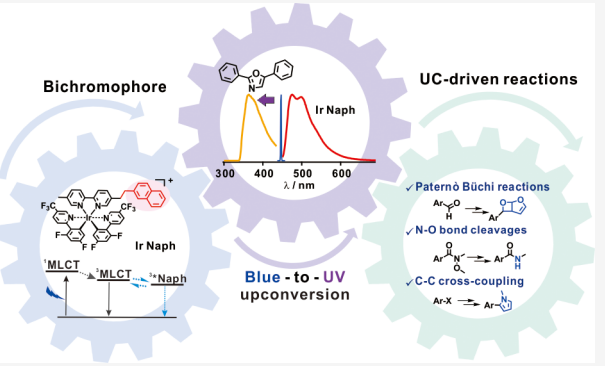

INTRODUCTION

Most photoredox reactions rely on monophotonic excitation, usually implying a linear dependence of reaction rates on excitation power.[1] Over the last decade, biphotonic processes received increasing attention in photoredox catalysis. Biphotonic reactions typically rely on the consecutive absorption of two photons per catalytic turnover and therefore feature a quadratic dependence on excitation power,[2] but at the so-called excitation power density threshold (I_{th}), they can crossover into a linear power dependence regime.[3] The development of new concepts to lower this threshold seems desirable for making biphotonic processes more amenable to photoredox catalysis.

Many different types of biphotonic processes have been uncovered,[2,4−11] among which sensitized triplet–triplet annihilation upconversion (sTTA-UC) is particularly promising. While upconversion has been intensively investigated from a photophysical perspective for applications in lighting and solar energy harvesting,[12−15] its use in photoredox catalysis is a relatively recent development.[16−25] Several non-catalytic photochemical reactions driven by upconversion have furthermore drawn interest.[26−29]

Blue-to-UV upconversion seems particularly attractive for photochemical applications because UV excitation sources are less available, typically less powerful, and less safe to handle than visible light-emitting diodes. UV irradiation can lead to photo-damage resulting from direct absorption by substrates rather than photocatalysts, and sufficiently deep penetration into reaction vessels can be hampered. Consequently, blue-to-UV upconversion is currently receiving substantial attention,[30−47] though applications in photoredox catalysis have yet remained scarce.[21,48−54] For photochemical applications, the upconversion system should be robust and operate with sufficient efficiency, for which there are several figures of merit.[55] Besides the maximum upconversion efficiency reachable under high irradiance, the excitation power density threshold (I_{th}), at which the upconversion changes from the initial quadratic power dependence to a linear regime, is of key interest for lowering the needed irradiation power.[56,57]

Received: March 17, 2023
Published: May 15, 2023

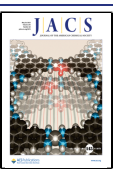

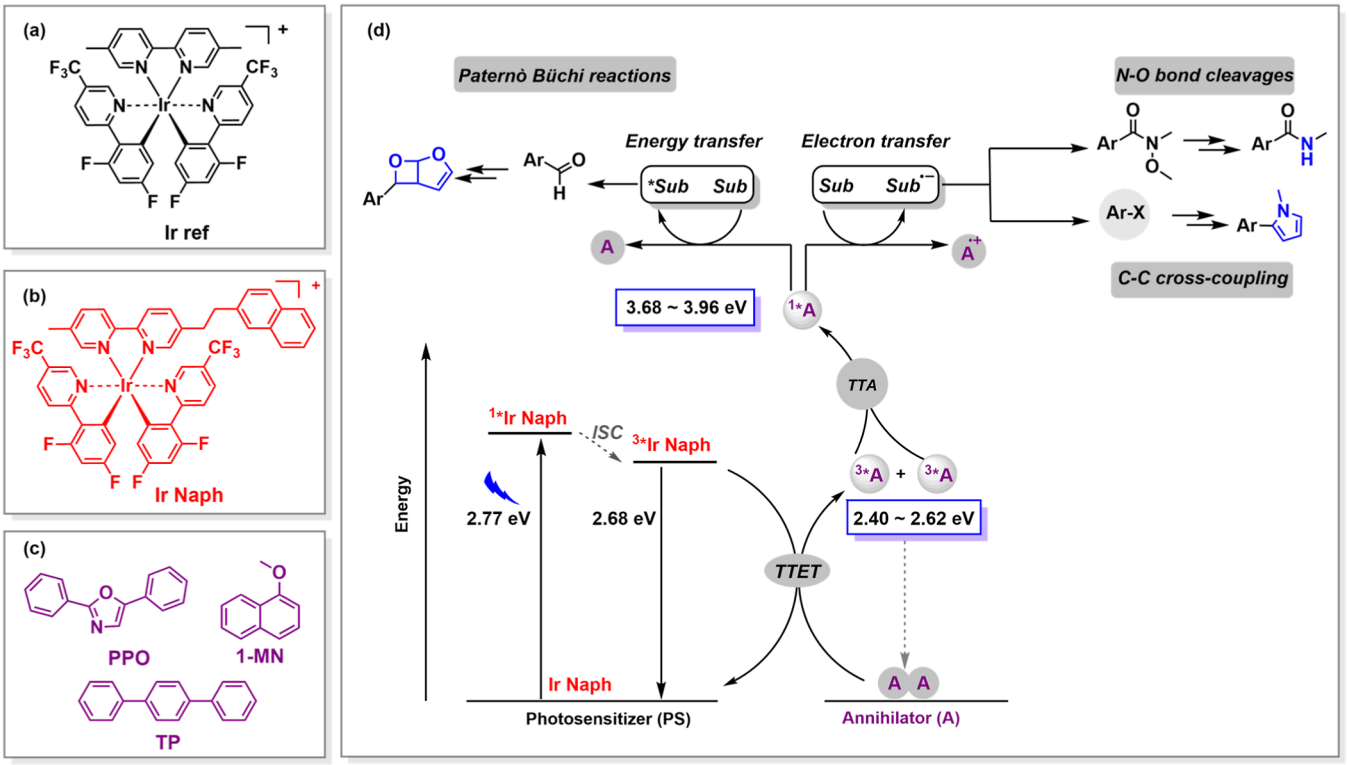

Figure 1. Molecular structures of (a) reference complex **Ir ref**, (b) bichromophore **Ir Naph**, and (c) the annihilators used in this study: 2,5-diphenyloxazole (**PPO**), 1-methoxynaphthalene (**MN**), and *p*-terphenyl (**TP**). (d) Illustration of sensitized triplet−triplet annihilation upconversion (sTAA-UC) and its applications in photocatalysis, either via energy- or electron transfer from the fluorescent singlet-excited state of the annihilator. ISC: intersystem crossing; TTET: triplet−triplet energy transfer; TTA: triplet−triplet annihilation; Sub: substrate.

A long triplet excited-state lifetime of the sensitizer is beneficial to lower the excitation power density threshold for upconversion.[58] To elongate the respective lifetimes in metal-based sensitizers, organic chromophores with energetically close-by triplet states have been covalently attached to many different metal complexes,[59,60] often resulting in reversible triplet−triplet energy transfer.[61,62] This so-called "triplet reservoir effect" is a well-known strategy for obtaining very long-lived emissive triplet states,[63] and in a handful of prior studies, such metal−organic bichromophores have already been successfully used for upconversion.[27,64−66] However, we are unaware of prior studies that have investigated systematically their impact on the excitation power density threshold with different annihilators, and so far, blue-to-UV upconversion has not been investigated with metal−organic bichromophores. Pyrene is a well-suited triplet reservoir for Ru^{II} polypyridine complexes with triplet energies around 2.1 eV,[67−70] but when aiming at blue-to-UV upconversion, a higher triplet energy is advantageous. Cyclometalated Ir^{III} complexes such as **Ir ref** (Figure 1a) fulfill this requirement with triplet energies near 2.7 eV,[71,72] but this calls for a different triplet reservoir.[73−75] Naphthalene (**Naph**) was identified as an energetically matching partner to obtain a substantially longer-lived triplet state in the bichromophore of Figure 1b (**Ir Naph**).[62] At the same time, all benefits offered by the Ir^{III} complex remain exploitable, in particular, its absorption tailing into the blue spectral range, high photostability, and high efficiency for intersystem crossing. In combination with the three annihilators shown in Figure 1c, the **Ir Naph** bichromophore consistently gives lower excitation power density thresholds (I_{th}) than the **Ir ref** compound. This finding supports our hypothesis that bichromophores and the triplet reservoir effect can be beneficial for lowering I_{th} and represents one key novelty of our study.

Ir Naph sensitizes the lowest triplet states of the three annihilators shown in Figure 1c with energies between 2.40 and 2.62 eV (lower half of Figure 1d), resulting in fluorescent singlet-excited states with energies between 3.68 and 3.96 eV after upconversion. The combination of **Ir Naph** with **PPO** emerged as the optimal sensitizer/annihilator couple for photochemical investigations. The singlet-excited state of **PPO** formed after upconversion engaged in both electron and energy transfer processes in three fundamentally different types of chemical reactions (upper half of Figure 1d). The Paternò−Büchi reaction between two benzaldehydes and furan usually relies on 365 nm (3.40 eV) irradiation,[76] whereas here it was accomplished with 447 nm light (2.77 eV), owing to energy transfer from the upconverted **PPO** state at 3.68 eV. N−O bond cleavage reactions of three Weinreb amides, normally requiring UV activation,[77] and one thermodynamically demanding C−C coupling reaction were driven by blue light, as a result of the strongly reducing character of the formed **PPO** singlet-excited state. The proof-of-concept that several different chemical reaction types, some relying on energy transfer and others functioning on the basis photoinduced electron transfer, become accessible after blue-to-UV upconversion represents another key novelty of our study. In combination with the bichromophore strategy to lower excitation power density thresholds, this represents a significant conceptual advance of upconversion-driven UV photocatalysis.

https://doi.org/10.1021/jacs.3c02609
J. Am. Chem. Soc. 2023, 145, 11402−11414

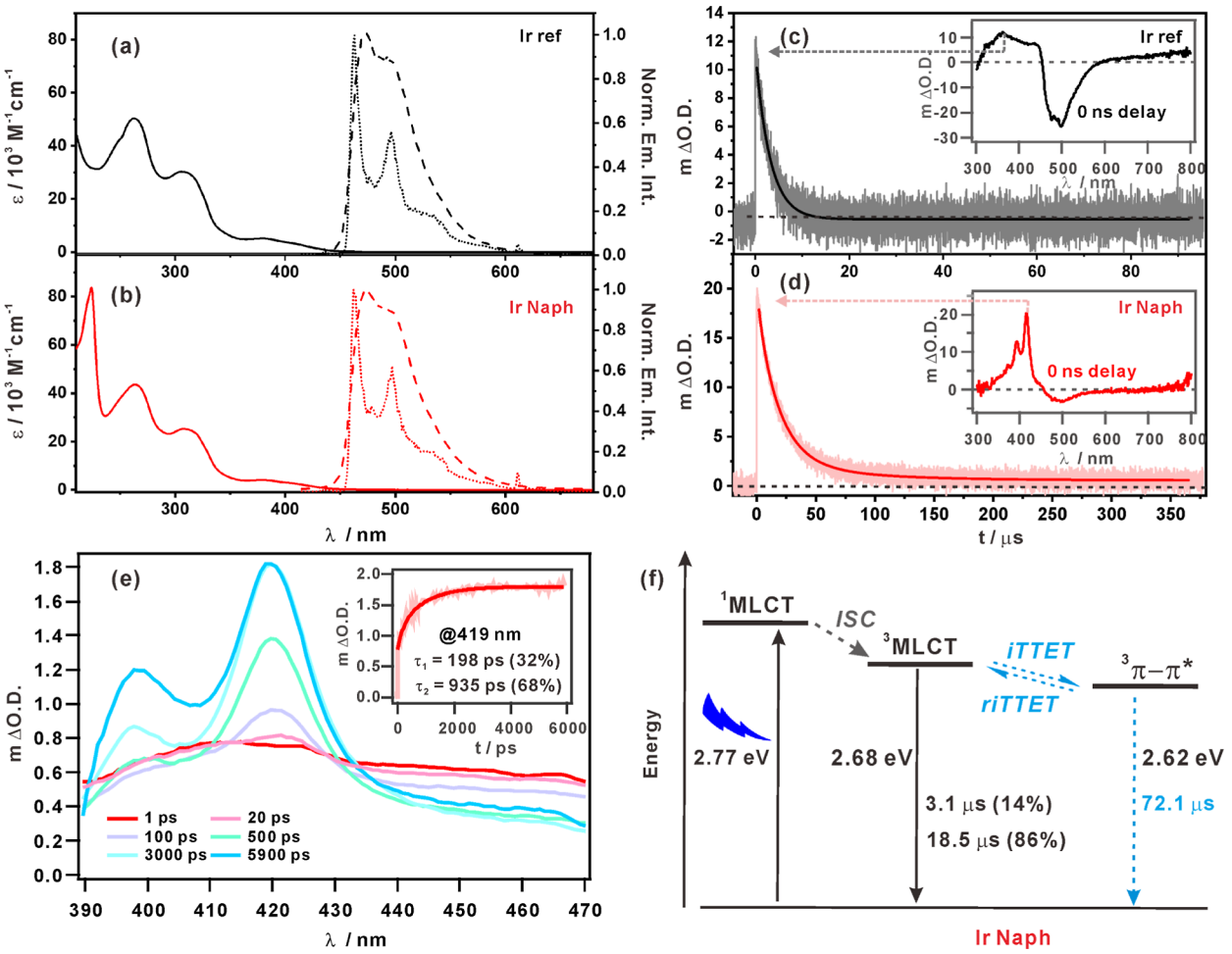

Figure 2. Photophysical properties of the Ir-based sensitizers from Figure 1. (a,b) UV−vis absorption spectra of **Ir ref** (solid black trace) and **Ir Naph** (solid red trace), along with normalized luminescence spectra of **Ir ref** (dashed black trace) and **Ir Naph** (dashed red trace) in dry deaerated CH_3CN at 293 K, excited at 405 nm. Luminescence spectra of **Ir ref** (black dotted trace) and **Ir Naph** (red dotted trace) in 2-methyl-THF at 77 K, after excitation at 405 nm. (c,d) Decays of the excited-state absorption signals for 30 μM **Ir ref** (at 360 nm, gray trace) and 30 μM **Ir Naph** (at 418 nm, pale red trace) in dry, deaerated MeCN at 293 K after excitation at 415 nm with laser pulses of ~10 ns duration. Insets: transient absorption spectra measured directly after 415 nm excitation of 30 μM **Ir ref** (black trace) and 30 μM **Ir Naph** (red trace) under identical conditions. (e) UV−vis transient absorption spectra of 1.34 mM **Ir Naph** in aerated CH_3CN at 293 K, recorded at different time delays following excitation at 375 nm. Inset: Temporal evolution of the signal at 419 nm. (f) Energy-level diagram including the key photophysical processes upon excitation of **Ir Naph**. ISC: intersystem crossing; iTTET: intramolecular triplet−triplet energy transfer; riTTET: reverse intramolecular triplet−triplet energy transfer.

RESULTS AND DISCUSSION

Photophysical Characterization of the Triplet Sensitizers. **Ir ref** and the bichromophore **Ir Naph** were synthesized and characterized as described in the Supporting Information (Sections 2.3 and 2.4). The UV−vis absorption spectra of **Ir ref** and **Ir Naph** (Figure 2a,b) are very similar to one another and differ mainly by an additional band at 224 nm in **Ir Naph**, which is attributable to $\pi-\pi^*$ transitions on the naphthalene unit. At the excitation wavelength used for the upconversion experiments (447 nm), both compounds have a molar extinction coefficient of ~350 M^{-1} cm^{-1}.

From the luminescence spectra at 77 K, an energy of 2.68 eV is estimated for the emissive triplet excited state located on the Ir^{III} complex. The photoluminescence quantum yields in deaerated CH_3CN at 293 K are roughly 80% for both **Ir ref** and **Ir Naph** (Supporting Information Section 7). Evidently, the presence of the naphthalene moiety does not negatively affect the luminescence behavior, likely because the lowest triplet excited state of naphthalene decays 2−3 orders of magnitude more slowly than the emissive excited state of the Ir^{III} complex.[78] The luminescent excited states of cyclometalated Ir^{III} complexes of this type commonly have mixed metal-to-ligand charge transfer (MLCT) and intraligand character,[79,80] but for simplicity, we use only the MLCT label shown in Figure 2f and throughout the entire article.

The luminescence of **Ir ref** decays mono-exponentially with a lifetime of 3.1 μs in deaerated CH_3CN at 293 K, whereas **Ir Naph** shows a bi-exponential luminescence decay with 3.1 μs (14%) and 18.5 μs (86%) under identical conditions. In addition to the spectral features seen for **Ir ref**, the transient absorption spectrum of **Ir Naph** contains the spectral signature of the lowest triplet-excited state of naphthalene (narrow bands at 419 and 397 nm in the inset of Figure 2d).[81] This confirms that the anticipated intramolecular triplet−triplet energy transfer (iTTET) from the initially excited iridium(III) complex to the appended naphthalene unit occurs (Figure 2f). The transient absorption signal at 418 nm decays in a tri-exponential fashion, comprising the abovementioned decay

https://doi.org/10.1021/jacs.3c02609
J. Am. Chem. Soc. 2023, 145, 11402−11414

components of 3.1 and 18.5 μs seen already in the luminescence decay of **Ir Naph** (Figure S5b), along with a third decay component featuring a lifetime of 72.1 μs. The latter is attributable to the inherent decay of triplet-excited naphthalene, for which lifetimes around 100 μs and longer have been reported,[78] whereas the 3.1 μs decay component is evidently due to the emissive excited state of the iridium(III) complex. The remaining 18.5 μs decay component is attributed to repopulation of the emissive state on the Ir^{III} complex from the dark $^3\pi-\pi^*$ state of the naphthalene unit, and it reflects both the kinetics of the inherent $^3\pi-\pi^*$ decay and the kinetics of reverse iTTET. Analogous results have been obtained previously for Pt^{II}-anthracene and Ru^{II}-perylene bichromophores,[82−84] and the similarity of their multi-exponential luminescence decay behavior to that observed for thermally activated delayed fluorescence has been noted.[82]

The reaction rate for iTTET can be determined by transient absorption experiments with sub-nanosecond time resolution (Figure 2e). Following pulsed excitation of **Ir Naph** at 375 nm, the spectrum recorded with a time delay of 1 ps (red trace in Figure 2e) is rather nondescript but features an absorption maximum near 410 nm, attributable to the initially excited Ir^{III} complex.[5] At this point, population of the naphthalene $^3\pi-\pi^*$ excited state is minimal. After 20 ps (pink trace), the growth of a signal at 419 nm becomes apparent, reaching its maximum intensity after 3000 ps (turquoise trace). Together with the vibrational sideband at 397 nm, the absorption band at 419 nm represents the diagnostic spectral signature of the naphthalene-centered $^3\pi-\pi^*$ excited state, as noted above (inset of Figure 2d). From the kinetic trace at 419 nm (inset of Figures 2e and S7), time constants of 198 and 935 ps for iTTET were extracted. The bi-exponential nature of this kinetic trace is tentatively attributed to the presence of different conformers.

Temperature-dependent luminescence experiments with **Ir Naph** demonstrate that reverse iTTET becomes increasingly important as the temperature rises (Figure S6 and Table S1), and from an Arrhenius-type analysis, it follows that the energy gap between the emissive excited state of the Ir^{III} complex and the naphthalene $^3\pi-\pi^*$ state is roughly 0.1 eV. This finding is in line with the experimentally determined energy of the emissive excited state (2.68 eV) of **Ir Naph** and the known triplet energy (2.62 eV) of naphthalene.[85]

Photophysical Properties of the Annihilators. All three annihilators used in this work (Figure 1c) are known compounds with triplet energies between 2.40 and 2.62 eV (Table 1)[85] and energies of the fluorescent singlet-excited states ranging from 3.68 to 3.96 eV. Consequently, bimolecular TTET from the emissive excited state of both **Ir ref** and **Ir Naph** (at 2.68 eV, Figure 2f) to all three annihilators is expected to be exergonic, but for **1-MN** and **TP**, the driving force is small. All three annihilators fluoresce in the UV range with high quantum yields (ϕ), thus fulfilling a key prerequisite for blue-to-UV upconversion.

Table 1. Photophysical Properties of the Used Annihilators

compound	$E(T_1)^a$/eV	$E(T_1)$/μs	$E(S_1)^b$/eV	$\tau(S_1)^c$/ns	$\phi(S_1)^d$/%
PPO	2.40[e]	130[e]	3.68	1.6	97.2 ± 0.2
1-MN	2.59[f]	5500[g]	3.87	13.3	77.6 ± 0.8
TP	2.62[f]	450[g]	3.96	1.2	87.4 ± 0.2

[a]Energy of the lowest triplet excited state (T_1). [b]Energy of the lowest singlet excited state (S_1), determined from the intersection of absorption and normalized fluorescence spectra recorded from optically dilute samples at 293 K (Figure S1). [c]Fluorescence lifetime (Figure S2). [d]Fluorescence quantum yield in deaerated CH_3CN at 293 K. [e]From ref 90. [f]From ref 85. [g]From ref 78.

TTET from Ir ref and Ir Naph to the Three Annihilators. Transient absorption spectroscopy provides clear evidence for bimolecular TTET from **Ir Naph** to **PPO** (Figure 3a). A solution containing only **Ir Naph** (red trace) yields the same transient absorption spectrum as discussed above (inset of Figure 2d), with spectral features of the emissive Ir^{III} excited state and the naphthalene-localized $^3\pi-\pi^*$ state. In the presence of excess **PPO**, these spectral signatures remain observable only at very short delay time (blue trace in Figure 3a), whereas at long delay times (orange trace), the diagnostic spectrum of triplet-excited 2,5-diphenyloxazole (^{3}***PPO**) is detected.[34] Analogous experiments with **1-MN** and **TP** (Figures S18a and S20a) provide equally clear evidence for bimolecular TTET.[86−89]

Luminescence quenching experiments and Stern−Volmer analyses were used to determine the rate constants for bimolecular TTET (k_{TTET}) from **Ir Naph** or **Ir ref** to the three annihilators. Exemplary data are shown for the **Ir Naph**/**PPO** couple in Figure 3b; analogous data sets for all other sensitizer/annihilator combinations are in the Supporting Information (Section 5). Expectedly, the highest k_{TTET} values are obtained with **PPO** (Table 2) because the driving force for TTET is largest in this case, roughly 0.28 eV, compared to only 0.09 eV for **1-MN** and 0.06 eV for **TP** based on Figure 2f and Table 1. Steady-state luminescence quenching experiments provide similar k_{TTET} values as the time-resolved luminescence studies (Table S3).

The apparent rate constants for TTET determined from luminescence quenching experiments are consistently lower for **Ir Naph** than for **Ir ref**, and this difference becomes more obvious as the reaction free energy for TTET (ΔG_{TTET}) gets less negative from **PPO** to **1-MN** and **TP** (Table 2). This is likely attributable to the population of the naphthalene-based $^3\pi-\pi^*$ excited state at 2.62 eV (Figure 2f) in **Ir Naph**, from which TTET to the annihilator is less exergonic than from the emissive Ir^{III}-localized MLCT state at 2.68 eV (second series of ΔG_{TTET} values in Table 2). The ^{3}MLCT and $^3\pi-\pi^*$ states of the bichromophore are in equilibrium with each other as discussed above, hence the luminescence quenching experiments monitor their joint depopulation. In principle, transient absorption spectroscopy could be used to probe bimolecular TTET from the naphthalene subunit to the annihilators, but such experiments are hampered by the fact that the absorptions of the respective triplet donors and acceptors overlap spectrally.

The efficiency for TTET (ϕ_{TTET}) in the presence of excess annihilator, as relevant under upconversion conditions, can be pushed to nearly 100% in all cases (Table 2). In the presence of 1 mM **PPO**, time-resolved luminescence quenching experiments indicate that 94% of the emissive excited state of **Ir ref** are quenched by TTET, whereas for **Ir Naph**, quenching by TTET is 99% efficient under identical conditions. Despite similar k_{TTET} values in these two specific cases, a higher TTET efficiency is reached for **Ir Naph** owing to the substantially longer lifetimes of the triplet reservoir (18.5 and 72.1 μs) in comparison to the luminescent ^{3}MLCT state of the Ir^{III} complex (3.1 μs). With **1-MN** and **TP**, higher concentrations (5 mM instead of 1 mM) are needed to reach similar quenching efficiencies due to the lower driving forces for TTET.

https://doi.org/10.1021/jacs.3c02609
J. Am. Chem. Soc. 2023, 145, 11402−11414

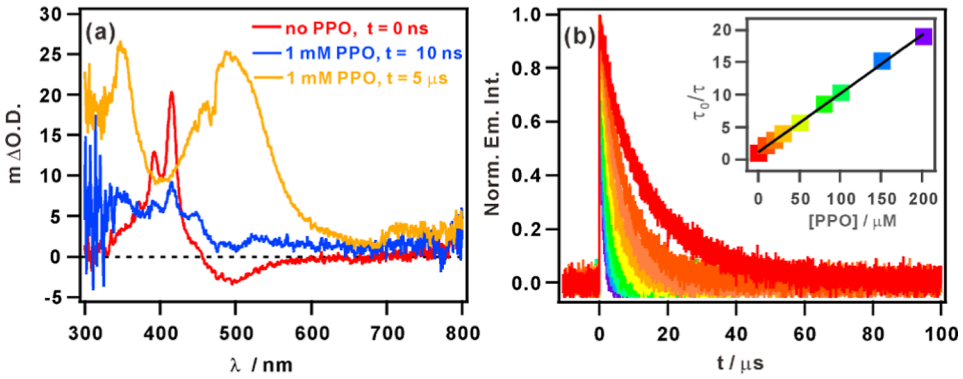

Figure 3. (a) Transient absorption spectra measured after 415 nm excitation of a 30 μM solution of **Ir Naph** in the absence of **PPO** (red trace) and with 1 mM **PPO** (orange and blue traces) in dry, deaerated MeCN at 293 K using laser pulses of ~10 ns duration. The signals were time-integrated over 200 ns without delay (red trace) and with time delays of 10 ns (blue trace) and 5 μs (orange trace). (b) Luminescence decays of 30 μM **Ir Naph** in dry deaerated MeCN at 293 K in the absence and in the presence of different concentrations of **PPO**. Excitation occurred at 415 nm, detection at 470 nm. Inset: Stern–Volmer plot based on the luminescence decays from the main plot.

Table 2. TTET Driving Forces, Rate Constants, and Efficiencies

	ΔG_{TTET}[a]/eV		k_{TTET}/10^9 $M^{-1}s^{-1}$		ϕ_{TTET}[b]/%	
annihilator	Ir ref	Ir Naph	Ir ref	Ir Naph	Ir ref	Ir Naph
PPO	−0.28	−0.28/−0.22	5.65	5.49	94	99
1-MN	−0.09	−0.09/−0.03	5.88	3.97	99	100
TP	−0.06	−0.06/0.00	1.46	0.59	96	98

[a]Reaction free energies for TTET estimated on the basis of the triplet energies in Figure 2f (^{3}MLCT energy and $^3\pi$–π^* energy) and Table 1. [b]Efficiency calculated using $(\tau_0-\tau)/\tau_0$, where τ_0 is the natural emission lifetime and τ is the luminescence lifetime (eq S1) measured in the presence of a given annihilator concentration. c[**PPO**] = 1 mM; c[**1-MN**] = 5 mM; c[**TP**] = 5 mM.

Blue-to-UV Upconversion. Upon selective excitation of **Ir Naph** at 447 nm in the presence of excess **PPO**, upconversion luminescence from the singlet-excited state of the annihilator and prompt MLCT emission from the sensitizer are both observable (Figure 4a). The maximum of the upconverted fluorescence is at 360 nm, corresponding to a pseudo anti-Stokes shift of 0.67 eV with respect to the excitation wavelength (447 nm). The delayed nature of the upconversion fluorescence manifests readily in a pulsed experiment (inset of Figure 4a). The decay of this delayed fluorescence is bi-exponential with time constants of 14.6 μs (65%) and 57.1 μs (35%) for 30 μM **Ir Naph** and 1 mM **PPO** in CH_3CN at 293 K (Figure S16d). These time constants are roughly a factor of two shorter than those extracted from the decay of the lowest triplet excited state of the **PPO** annihilator [29.9 μs (53%) and 136 μs (47%)] under identical conditions. This approximate factor-of-two discrepancy between upconversion luminescence decays and annihilator triplet excited-state decays has been previously found by other investigators in different systems[17] and is encountered here for all six sensitizer/annihilator couples (Figures S16–S21).

Excitation Power Density Threshold I_{th} and Upconversion Efficiency $\phi_{sTTA\text{-}UC}$. The upconverted annihilator fluorescence and the prompt sensitizer emission were recorded as a function of laser excitation power between 6.7 and 433.5 mW (Figure 4b,c), which corresponds to power densities ranging from roughly 0.2 to 16.0 W·cm^{-2} given the beam size of the employed laser (Supporting Information Section 1). For the **Ir Naph**/**PPO** couple, the integrated upconversion luminescence intensity depends quadratically on the excitation power density (red trace in Figure 4d) up to a value of 0.71 ± 0.05 W·cm^{-2}, manifesting in a slope of 2.04 in the respective double-logarithmic representation. Beyond this threshold value (I_{th}, vertical red dotted line in Figure 4d),[12,90,91] the slope decreases to 1.12, indicating that the strong annihilation limit is reached, where the upconversion luminescence intensity depends linearly on excitation power density.[3,58] The prompt sensitizer MLCT emission intensity follows the expectable linear dependence over the full range of excitation power densities used (red trace in Figure 4e). When performing the same experiment with **Ir ref** instead of **Ir Naph** as the sensitizer (black-colored data sets in Figure 4d,e; raw data in Figure S22), the excitation power density threshold (I_{th}) is reached at 1.4 ± 0.1 W·cm^{-2}, roughly double the value determined for the bichromophore sensitizer. When decreasing the **PPO** annihilator concentration from 1 to 0.2 mM while keeping the sensitizer concentration constant at 30 μM (Figure S23), the excitation power density thresholds increase because the concentration of triplet-excited annihilators becomes lower.[92−94] However, the I_{th} value obtained with **Ir Naph** (1.6 ± 0.2 W·cm^{-2}) remains substantially below that for **Ir ref** (2.2 ± 0.2 W·cm^{-2}). When using **1-MN** or **TP** instead of **PPO** as annihilators (Figures S24 and S25), the **Ir Naph** bichromophore also gives substantially lower power density thresholds than **Ir ref** (Table 3). The finding that the metal–organic bichromophore with its very long-lived triplet reservoir gives consistently lower I_{th} values than an ordinary sensitizer (Table 3) is a key result of this study.

A quantitative analysis of the excitation power density threshold dependence on exact sensitizer/annihilator properties, as discussed previously,[56,92−95] is hampered by the overall complexity of our upconversion systems (Supporting Information Section 9), particularly with **1-MN** and **TP**, for which bimolecular reverse TTET from the annihilators to the sensitizer complicates the situation (see below and Figure S27). However, in the case of the **PPO** annihilator, the physical origin of the lower I_{th} values for **Ir Naph** in comparison to that for **Ir ref** can be rationalized by the considerably longer excited-state lifetime of the sensitizer (Figure 2d). The TTET rate constants are similar for both sensitizers (Table 2), but at any given annihilator concentration, the τ_0/τ and I_0/I ratios extracted from time-resolved

https://doi.org/10.1021/jacs.3c02609
J. Am. Chem. Soc. 2023, 145, 11402−11414

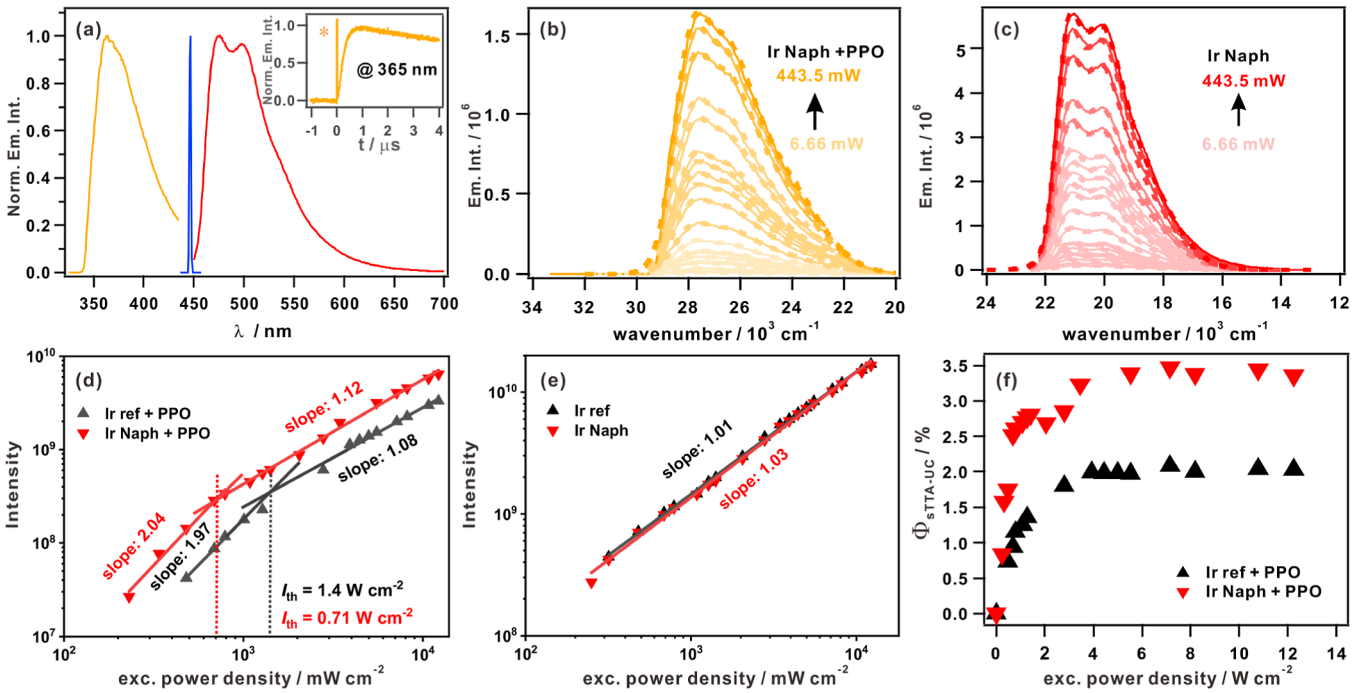

Figure 4. (a) Normalized upconversion luminescence spectrum of **PPO** (1 mM, yellow trace) sensitized by **Ir Naph** (30 μM) in dry deaerated MeCN at 293 K along with the prompt emission of **Ir Naph** (30 μM, red trace) in the absence of annihilator but otherwise identical conditions. The blue trace is the emission profile of the 447 nm cw laser. Inset: Temporal evolution of the upconversion fluorescence emitted by **PPO** (1 mM) at 365 nm following pulsed excitation of 30 μM **Ir Naph** at 415 nm. The asterisk marks laser stray light. (b) Delayed fluorescence of **PPO** (1 mM) sensitized by **Ir Naph** (30 μM) in dry deaerated MeCN at 293 K following continuous excitation at 447 nm with various laser powers. (c) Prompt emission of **Ir Naph** (30 μM) measured under identical conditions as the spectra in (b), but in the absence of **PPO**. The **Ir Naph** emission intensity was attenuated with a neutral-density filter with an absorbance of 0.94 at 474 nm. (d) Double logarithmic plot of the upconversion luminescence intensity of **PPO** as a function of excitation power density; the black triangles represent data recorded with **Ir ref** as the sensitizer (data from Figure S22a), whereas the red triangles stand for data recorded with **Ir Naph** as the sensitizer (data from (b)). (e) Double logarithmic plot of the prompt luminescence intensity of **Ir ref** (black triangles, data from Figure S22b) and **Ir Naph** (red triangles, data from (c)) as a function of excitation power density, measured in the absence of **PPO**; the solid lines are fits to the experimental data. (f) Upconversion luminescence quantum yield as a function of excitation power density based on the data in (b,c), and Figure S22.

Table 3. Upconversion Properties of the Different Sensitizer/Annihilator Combinations

			$\phi_{sTTA\text{-}UC}$[c]/%		I_{th}[d]/W·cm^{-2}	
annihilator	λ_{em}[a]/nm	ΔE[b]/eV	Ir ref	Ir Naph	Ir ref	Ir Naph
PPO	360	0.67	2.03	3.47	1.4 ± 0.1[e]	0.71 ± 0.05[e]
					2.2 ± 0.2[f]	1.6 ± 0.2[f]
1-MN	337	0.91	0.33	0.28	3.5 ± 0.3	2.2 ± 0.2
TP	340	0.88	0.69	0.53	1.3 ± 0.1	0.90 ± 0.05

[a]Wavelength of the upconversion luminescence band maximum. [b]Pseudo anti-Stokes shift, defined as the energy difference between the excitation wavelength (447 nm) and the wavelength of the upconversion luminescence band maximum. [c]Quantum yield for sensitized triplet−triplet annihilation upconversion, determined using eq S2. Conditions: c[sensitizer] = 30 μM, c[**PPO**] = 1 mM; c[**1-MN**] = 5 mM; c[**TP**] = 5 mM. [d]Excitation power density threshold. [e]c[**PPO**] = 1 mM. [f]c[**PPO**] = 0.2 mM. See Section 7 of the Supporting Information for details.

and steady-state luminescence quenching experiments are a factor of 3.3−4.4 higher for **Ir Naph** than for **Ir ref** (Figures S11−S13). This indicates that considerably lower concentrations of **PPO** are needed in combination with **Ir Naph** to reach the same amount of quenching as with **Ir ref**, and this in turn is in line with a lower I_{th} value for the bichromophore.

The excitation power density thresholds determined for our sensitizer/annihilator couples (Table 3) compare reasonably well to previously reported I_{th} values for other blue-to-UV upconversion systems (Table S5) and lie somewhere in the middle between the best and worst performers. The main point here is not to establish new record I_{th} values, but to demonstrate that bichromophores, which benefit from a triplet reservoir effect, are useful to lower the excitation power density thresholds. This proof-of-principle is now made, and we are unaware of previous reports that have explored and successfully demonstrated the usefulness of this specific concept. Optimizing I_{th} is of significant interest, for example, in the context of solar energy conversion,[12,96,97] but also to use LEDs instead of lasers in photocatalysis.

Aside from the excitation power threshold, the upconversion efficiency ($\phi_{sTTA\text{-}UC}$) is a key figure of merit.[55,95,98,99] To determine $\phi_{sTTA\text{-}UC}$ for our systems, the ratios of upconversion luminescence intensity and the prompt sensitizer emission intensity of a reference solution containing no annihilator were measured as a function of the excitation power density (Figures 4b,c and S22−S25), to provide data sets such as those in Figure 4f (see Supporting Information Section 7 for details).

https://doi.org/10.1021/jacs.3c02609
J. Am. Chem. Soc. 2023, 145, 11402−11414

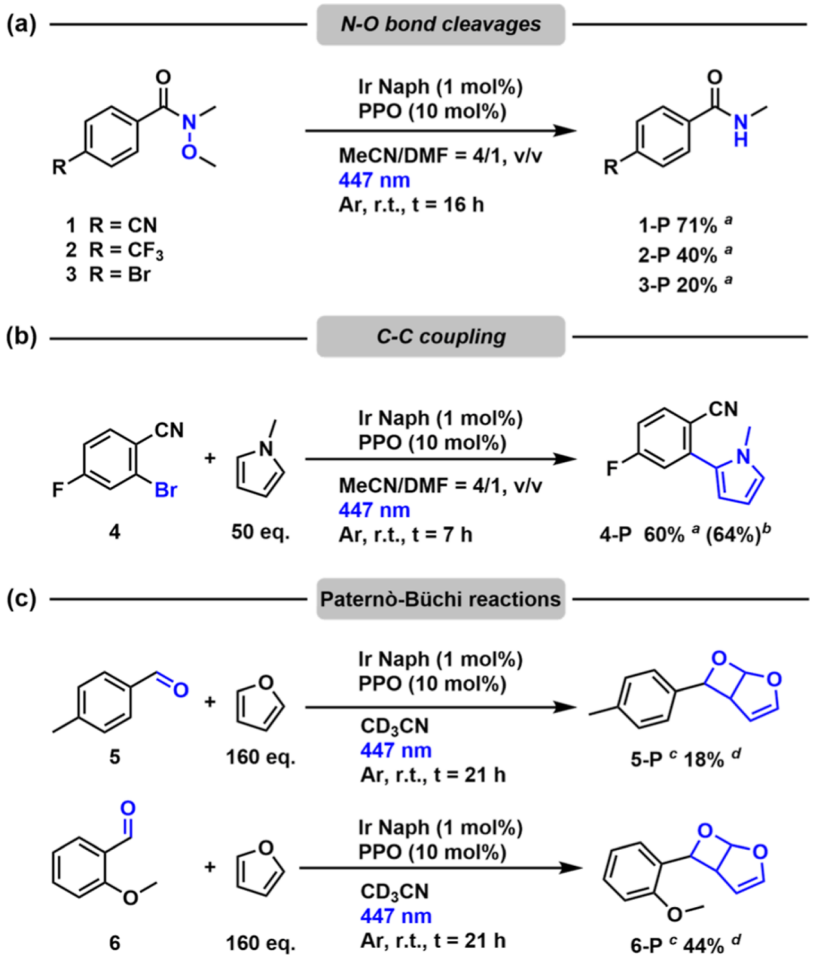

Figure 5. Photoreactions performed with the **Ir Naph**/**PPO** upconversion system. [a]Isolated yields; [b] ^{19}F NMR yield using 4-fluorotoluene as internal standard; [c]exo-product obtained selectively; [d] ^{1}H NMR yield using trimethyl(phenyl)silane as internal standard.

For the **Ir Naph**/**PPO** couple, $\phi_{sTTA\text{-}UC}$ is roughly 70% higher than for the **Ir ref**/**PPO** combination (Table 3), suggesting that the bichromophore concept and the triplet reservoir effect might be generally helpful to boost $\phi_{sTTA\text{-}UC}$ in addition to I_{th}. However, with the other two investigated annihilators (**1-MN** and **TP**), the upconversion efficiencies are lower with **Ir Naph** than with **Ir ref** (Table 3), which we attribute to reverse TTET from the annihilator to the sensitizer. Several observations support this conclusion, as discussed briefly in the following. First, the driving-forces for TTET to these annihilators are very small (ΔG_{TTET} in Table 2), particularly for **Ir Naph**, hence reverse TTET is thermodynamically viable. Time-gated luminescence experiments provide direct evidence for reverse TTET (Figures S18−S21) in the form of delayed sensitizer MLCT luminescence. Bimolecular reverse TTET is likely responsible for the finding that the upconversion excitation power dependence deviates substantially from quadratic behavior already in the low-power regime, yielding slopes closer to 1.8 instead of 2.0 (Figures S24e/S25e).[91,100] Given the presence of the naphthalene-based $^{3}\pi-\pi^{*}$ state at 2.62 eV in **Ir Naph** (Figure 2f), reverse TTET from the annihilator to this excited state is more facile than to the 0.06 eV higher-lying ^{3}MLCT state of the Ir^{III} complex. On this basis, the lower upconversion efficiencies obtained for **Ir Naph** in comparison to **Ir ref** when using **1-MN** and **TP** as annihilators (Table 3) can be rationalized. With **TP**, an unusual excitation power dependence of the upconversion efficiency ($\phi_{sTTA\text{-}UC}$) is obtained (Figure S25g), likely as a result of particularly prominent reverse TTET in this case.[100,101]

The maximally achievable upconversion quantum yield of the **Ir Naph**/**PPO** couple compares favorably to many previously reported blue-to-UV upconversion systems (Table S5), for which $\phi_{sTTA\text{-}UC}$ has often been in the range of 1−5% until now, though improved performance became possible recently in several cases.[30,41,42,47,92] The **Ir Naph**/**PPO** couple emerged as the best upconversion system from our study both regarding $\phi_{sTTA\text{-}UC}$ and I_{th}, and furthermore, this combination turned out to be remarkably photostable (Figure S10). Over 6 h of irradiation at 447 nm with a 451 mW cw-laser, only a 25% decrease of the upconversion luminescence intensity was observed, making the **Ir Naph**/**PPO** couple promising for applications in UV photocatalysis. The inherent photostability in neat solution is often lower than under catalytic conditions, particularly when long-lived triplet excited states are involved.[102] Strongly quenched systems avoid deleterious side reactions, and when using elevated sensitizer/annihilator concentrations, photo-irradiation periods longer than 6 h are expected to become unproblematic for our upconversion system (Supporting Information page S95).

UV Photoreactions Driven by Upconversion. Storing roughly 3.68 eV of excitation energy (Table 1), the fluorescent singlet-excited state of 2,5-diphenyloxazole (^{1}***PPO**) is a fairly strong reducing agent with an oxidation potential of −2.2 V vs SCE (Supporting Information Section 10).[103,104] Conse-

https://doi.org/10.1021/jacs.3c02609
J. Am. Chem. Soc. 2023, 145, 11402−11414

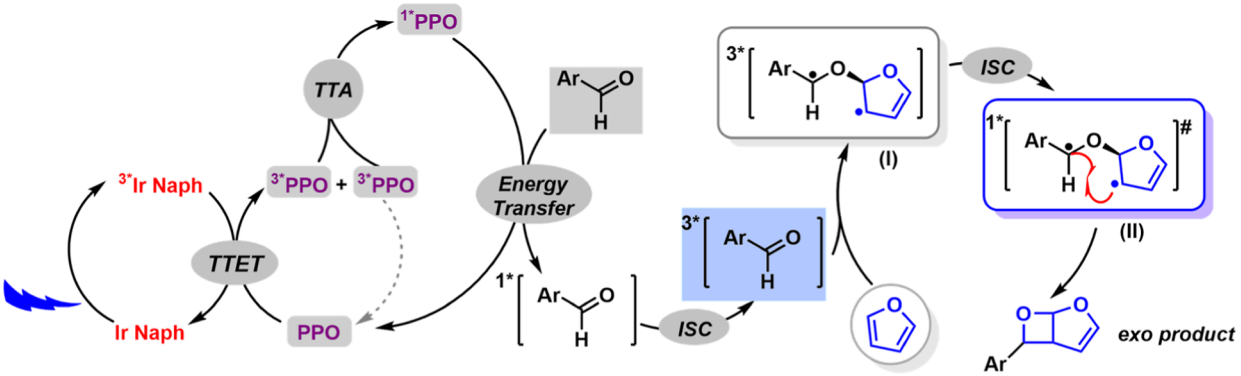

Figure 6. Proposed mechanism for the Paternò–Büchi reactions from Figure 5c, involving the upconversion system (left) and a previously proposed pathway for the respective [2 + 2] cycloaddition reaction (right).[76,105] Energy transfer from the fluorescent singlet-excited state of the PPO annihilator to the aldehyde substrate can be either radiative or nonradiative. Förster resonance energy transfer (FRET) is plausible in the employed one-pot reaction setup, in which all components (upconversion system and substrates) are together in the same solution. The proposed reaction sequence converts a low-energy triplet (^{3}*PPO, storing 2.4 eV) into a higher-energy triplet (^{3}*ArCHO, storing 3.1 eV), which is an uncommon form of photochemical upconversion.

quently, it seemed attractive to explore whether ^{1}*PPO, formed via upconversion of visible light, can catalyze chemical reductions that previously required UV irradiation, such as the recently reported reductive N–O bond cleavage reactions of Weinreb amides (Figure 5a).[77] The reduction potential of these substrates is tunable through variation of the substituent R in para-position to the protected amide group (Table S7). For the three specific examples investigated here, the obtainable product yields correlated with the substrate reduction potential (Figure 5a, Table S7), suggesting that the initial photoinduced electron transfer step from ^{1}*PPO to the substrate is indeed a performance-limiting factor. Following this initial elementary process enabled by upconversion, the deprotection of the Weinreb amide is expected to proceed along the same reaction pathway as postulated for direct UV excitation (Scheme S1).[77] Substrate **1** is converted to product **1-P** in 71% yield under 447 nm irradiation of 1 mol % **Ir Naph** as the sensitizer and 10 mol % **PPO** as the annihilator. Control experiments confirm that both upconversion components (sensitizer, annihilator) and light are indispensable for this reaction (Table S8 and Figures S30–S36), and only a minor background reactivity (17% yield of **1-P**) is observed when the annihilator is missing (Supporting Information Section 12.1). Substrates **2** and **3** have slightly more negative one-electron reduction potentials than substrate **1** (Table S7), and the obtainable N–O bond cleavage yields are markedly lower (40% for **2-P**, 20% for **3-P**; Supporting Information Sections 12.2 and 12.3). For substrates **1** and **2**, **Ir Naph** and **Ir ref** are similarly good sensitizers under the conditions used for these experiments, whereas for substrate **3**, **Ir ref** performs substantially more poorly (<6% yield, Table S10).

For the reductive debromination of substrate **4** (Figure 5b) followed by interception of the formed aryl radical by *N*-methylpyrrole (Supporting Information Section 12.4),[19,20] the difference in product yield (**4-P**) obtained with **Ir Naph** and **Ir ref** is substantial (64% vs 15%, Table S11). In a control experiment performed in the absence of **PPO**, 21% yield of the C–C coupling product **5-P** is obtained, and Stern–Volmer experiments indicate that substrate **4** quenches the **Ir Naph** emission with a rate constant of 3×10^6 M^{-1} s^{-1} (Figure S50), which is more than three orders of magnitude slower than TTET from **Ir Naph** to **PPO** (Table 2). Thus, it seems clear that the dominant reaction pathway in the complete upconversion system proceeds via TTET from **Ir Naph** to **PPO**, followed by upconversion to ^{1}*PPO and electron transfer from that upconverted state to the substrate (Supporting Information Section 12.4).

Aside from reacting via photoinduced electron transfer, ^{1}*PPO can furthermore be expected to serve as an energy donor, which could open new perspectives for energy transfer catalysis. Photoredox catalysis via upconversion is an emerging field,[18−22,27,54,106−108] whereas energy transfer catalysis via upconversion is yet very uncommon.[29,54,109] Two Paternò–Büchi model reactions (Figure 5c) were chosen to explore the concept of converting a lower energy triplet-excited state into a higher energy triplet-excited state. The [2 + 2] cycloaddition reaction of benzaldehydes with furan usually requires UV irradiation at 365 nm (3.40 eV)[76] because the energy of the reactive triplet-excited state of benzaldehydes is ca. 3.1 eV and light absorption commonly occurs via excitation of substantially higher-lying singlet-excited states.[78] Here, we aimed to populate the reactive triplet-excited state of two different benzaldehyde molecules via an upconversion process, using an input energy of 2.77 eV (447 nm) instead of 3.40 eV, anticipating that the spectral overlap between the (delayed) ^{1}*PPO fluorescence and the benzaldehyde absorption (Figure S29) would enable energy transfer from the upconversion system to the substrate (Figure 6).

The respective spectral overlap between donor emission and acceptor absorption is markedly better with substrate **6** than with substrate **5**. Consequently, it seems plausible that the higher yield of cycloaddition product **6-P** (44%, 49% conversion) in comparison to **5-P** (18%; 23% conversion) is largely attributable to this better spectral overlap and a higher molar extinction of **6-P** in the relevant spectral range (Figure S29). Control experiments performed for the two reactions shown in Figure 5c confirm that both upconversion components (sensitizer and annihilator) must be present and that blue light drives the UV photoreactions via upconversion (Tables S12 and S13). **Ir Naph** outperforms **Ir ref** as the sensitizer in both cases (Tables S12 and S13). Both [2 + 2] cycloaddition products are obtained predominantly in their exo form, as expected (right part of Figure 6).[76,105]

The key energy transfer step between ^{1}*PPO and the benzaldehyde substrates can occur both via radiative energy transfer and FRET. In a recent study, an upconverting

https://doi.org/10.1021/jacs.3c02609
J. Am. Chem. Soc. 2023, 145, 11402−11414

sensitizer-annihilator couple system for red-to-blue upconversion was spatially separated from a triplet photoreaction system, in which case radiative energy transfer involving delayed fluorescence from 9,10-diphenylanthracence and subsequent re-absorption of the upconverted light by a Ru^{II} complex occurred.[109] Similar two-compartment setups have been used previously for upconversion.[23,110] Here, we employed a simple one-pot reaction setup with all components present in the same solution, in which case FRET is possible as an important energy transfer mechanism between the upconversion system and the Paternò–Büchi photoreaction system. One possible pitfall in this strategy is reverse TTET from the photoreactive triplet-excited state of the benzaldehyde (^{3}***ArCHO** in Figure 6) to the annihilator (to form ^{3}***PPO**) or the sensitizer (to result in ^{3}***Ir Naph**). Using an excess of furan (Figure 5c), it has been possible to counteract this energy-wasting reaction pathway, such that a bimolecular C–C bond forming reaction has become possible, whereas previous related studies dealt mostly with simpler photoisomerization or photo–fragmentation reactions.[54,109] Paternò–Büchi and related cycloaddition reactions are regaining interest in current research,[111−116] and our proof-of-concept [2 + 2] cycloadditions shown in Figure 5c demonstrate that blue-to-UV upconversion can enable these reactions with visible light. Metal–organic bichromophores as sensitizers are useful for this purpose.

From a purely practical perspective, direct UV irradiation remains the most straightforward approach for the reactions shown in Figure 5. Advantages of the upconversion approach could result in systems, in which filter and photodegradation effects are prevalent, as discussed in the Introduction. These advantages will likely become more significant as increasingly shorter-wavelength UV radiation becomes accessible via upconversion.[46,47,54]

CONCLUSIONS

Three key discoveries emerge from this study: (1) metal–organic bichromophores can lower the excitation power density threshold for upconversion due to the triplet reservoir effect and substantially elongated excited-state lifetimes, enabling a linear power dependency at decreased excitation densities compared to ordinary sensitizers. (2) This concept enables blue-to-UV upconversion and subsequent exploitation of the upconverted light in photoredox and energy transfer catalysis, whereby not only photocleavage but also constructive C–C bond forming reactions are achievable. (3) Upconversion of lower energy triplets into higher energy triplet excited states can enable classical UV-dependent photoreactions of organic molecules, such as the Paternò–Büchi [2 + 2] cycloaddition.

The bichromophore strategy requires a fine energy-tuning between the triplet excited state of the emissive metal complex and the covalently attached triplet reservoir, in order for intramolecular TTET to be reversible.[63,117−119] A cyclometalated heteroleptic Ir^{III} complex and naphthalene are well-suited to create a long-lived triplet excited state in the deep blue region, roughly 0.6 eV higher in energy than most of the previously explored Ru^{II}-pyrene bichromophores,[59,60,68] which is essential for sensitization of blue-to-UV upconversion. While bimolecular TTET from the bichromophore to the annihilator is ideally associated with minimal energy loss in order to upconvert as deeply into the UV as possible,[48,54] a minimum driving force of 0.2 eV seems necessary, otherwise the overall upconversion efficiency is compromised. Two of the three investigated annihilators did not fulfill this requirement, and reverse TTET from these annihilators to the naphthalene triplet reservoir was identified as a detrimental process. The visible light-harvesting ability of the bichromophore is relatively modest, as often the case for cyclometalated iridium(III) complexes.[72,120]

Sensitized triplet–triplet annihilation creates higher-energy singlet-excited states, which can act as FRET donors. When using carbonyl compounds as FRET acceptors, those carbonyls can undergo efficient intersystem crossing to reactive triplet-excited states that lie at substantially higher energies than those of the initially excited sensitizer. Our work shows that energy-wasting TTET from these high-energy triplet-excited states back to the sensitizer-annihilator couple can be counteracted to the extent that bimolecular C–C bond-forming reactions become viable. This opens the door to classical carbonyl compound UV photochemistry with visible light, beyond simple Norrish type I and type II photofragmentations, but furthermore including diffusion-controlled bimolecular chemistry with substrates having high triplet energies. As traditional UV photochemistry of organic compounds is currently regaining interest in synthetically oriented research,[121,122] we hope that our study can contribute to developing new conceptual approaches to high-energy photochemistry.

ASSOCIATED CONTENT

Supporting Information

The Supporting Information is available free of charge at https://pubs.acs.org/doi/10.1021/jacs.3c02609.

Synthetic protocols and characterization data, description of equipment and methods, supplementary spectroscopic and electrochemical data, and photochemical reaction details (PDF)

AUTHOR INFORMATION

Corresponding Author

Oliver S. Wenger − *Department of Chemistry, University of Basel, Basel 4056, Switzerland;* orcid.org/0000-0002-0739-0553; Email: oliver.wenger@unibas.ch

Authors

Han Li − *Department of Chemistry, University of Basel, Basel 4056, Switzerland;* orcid.org/0000-0002-8916-3986

Cui Wang − *Department of Chemistry, University of Basel, Basel 4056, Switzerland*

Felix Glaser − *Department of Chemistry, University of Basel, Basel 4056, Switzerland;* orcid.org/0000-0002-6717-916X

Narayan Sinha − *Department of Chemistry, University of Basel, Basel 4056, Switzerland;* orcid.org/0000-0002-0406-5552

Complete contact information is available at: https://pubs.acs.org/10.1021/jacs.3c02609

Notes

The authors declare no competing financial interest.

ACKNOWLEDGMENTS

This work was funded by the Swiss National Science Foundation through grant number 200020_207329. C.W. thanks the Deutsche Forschungsgemeinschaft (DFG, German Research Foundation) for a Walter-Benjamin postdoctoral

fellowship (no. 496811278). We thank Dr. Christina Wegeberg for valuable input.

REFERENCES

(1) Marzo, L.; Pagire, S. K.; Reiser, O.; König, B. Visible-Light Photocatalysis: Does It Make a Difference in Organic Synthesis? *Angew. Chem., Int. Ed.* **2018**, *57*, 10034−10072.

(2) Glaser, F.; Kerzig, C.; Wenger, O. S. Multi-Photon Excitation in Photoredox Catalysis: Concepts, Applications, Methods. *Angew. Chem., Int. Ed.* **2020**, *59*, 10266−10284.

(3) Haefele, A.; Blumhoff, J.; Khnayzer, R. S.; Castellano, F. N. Getting to the (Square) Root of the Problem: How to Make Noncoherent Pumped Upconversion Linear. *J. Phys. Chem. Lett.* **2012**, *3*, 299−303.

(4) Chatterjee, A.; König, B. Birch-Type Photoreduction of Arenes and Heteroarenes by Sensitized Electron Transfer. *Angew. Chem., Int. Ed.* **2019**, *58*, 14289−14294.

(5) Connell, T. U.; Fraser, C. L.; Czyz, M. L.; Smith, Z. M.; Hayne, D. J.; Doeven, E. H.; Agugiaro, J.; Wilson, D. J. D.; Adcock, J. L.; Scully, A. D.; Gomez, D. E.; Barnett, N. W.; Polyzos, A.; Francis, P. S. The Tandem Photoredox Catalysis Mechanism of $[Ir(ppy)_2(dtb\text{-}bpy)]^+$ Enabling Access to Energy Demanding Organic Substrates. *J. Am. Chem. Soc.* **2019**, *141*, 17646−17658.

(6) Ghosh, I.; Ghosh, T.; Bardagi, J. I.; König, B. Reduction of Aryl Halides by Consecutive Visible Light-Induced Electron Transfer Processes. *Science* **2014**, *346*, 725−728.

(7) Goez, M.; Kerzig, C.; Naumann, R. An "All-Green" Catalytic Cycle of Aqueous Photoionization. *Angew. Chem., Int. Ed.* **2014**, *53*, 9914−9916.

(8) Kerzig, C.; Goez, M. Combining Energy and Electron Transfer in a Supramolecular Environment for the "Green" Generation and Utilization of Hydrated Electrons through Photoredox Catalysis. *Chem. Sci.* **2016**, *7*, 3862−3868.

(9) Coles, M. S.; Quach, G.; Beves, J. E.; Moore, E. G. A Photophysical Study of Sensitization-Initiated Electron Transfer: Insights into the Mechanism of Photoredox Activity. *Angew. Chem., Int. Ed.* **2020**, *59*, 9522−9526.

(10) Ayare, P. J.; Watson, N.; Helton, M. R.; Warner, M. J.; Dilbeck, T.; Hanson, K.; Vannucci, A. K. Molecular Z-Scheme for Solar Fuel Production via Dual Photocatalytic Cycles. *J. Am. Chem. Soc.* **2022**, *144*, 21568−21575.

(11) Fajardo, J.; Barth, A. T.; Morales, M.; Takase, M. K.; Winkler, J. R.; Gray, H. B. Photoredox Catalysis Mediated by Tungsten(0) Arylisocyanides. *J. Am. Chem. Soc.* **2021**, *143*, 19389−19398.

(12) Richards, B. S.; Hudry, D.; Busko, D.; Turshatov, A.; Howard, I. A. Photon Upconversion for Photovoltaics and Photocatalysis: A Critical Review. *Chem. Rev.* **2021**, *121*, 9165−9195.

(13) Bharmoria, P.; Bildirir, H.; Moth-Poulsen, K. Triplet−triplet annihilation based near infrared to visible molecular photon upconversion. *Chem. Soc. Rev.* **2020**, *49*, 6529−6554.

(14) Singh-Rachford, T. N.; Castellano, F. N. Photon upconversion based on sensitized triplet-triplet annihilation. *Coord. Chem. Rev.* **2010**, *254*, 2560−2573.

(15) Schloemer, T.; Narayanan, P.; Zhou, Q.; Belliveau, E.; Seitz, M.; Congreve, D. N. Nanoengineering Triplet−Triplet Annihilation Upconversion: From Materials to Real-World Applications. *ACS Nano* **2023**, *17*, 3259−3288.

(16) Pérez-Ruiz, R. Photon Upconversion Systems Based on Triplet−Triplet Annihilation as Photosensitizers for Chemical Transformations. *Top. Curr. Chem.* **2022**, *380*, 23.

(17) López-Calixto, C. G.; Liras, M.; de la Peña O'Shea, V. A.; Pérez-Ruiz, R. Synchronized biphotonic process triggering C-C coupling catalytic reactions. *Appl. Catal., B* **2018**, *237*, 18−23.

(18) Ravetz, B. D.; Pun, A. B.; Churchill, E. M.; Congreve, D. N.; Rovis, T.; Campos, L. M. Photoredox catalysis using infrared light via triplet fusion upconversion. *Nature* **2019**, *565*, 343−346.

(19) Glaser, F.; Kerzig, C.; Wenger, O. S. Sensitization-initiated electron transfer via upconversion: mechanism and photocatalytic applications. *Chem. Sci.* **2021**, *12*, 9922−9933.

(20) Glaser, F.; Wenger, O. S. Sensitizer-controlled photochemical reactivity via upconversion of red light. *Chem. Sci.* **2023**, *14*, 149−161.

(21) Majek, M.; Faltermeier, U.; Dick, B.; Pérez-Ruiz, R.; Jacobi von Wangelin, A. Application of Visible-to-UV Photon Upconversion to Photoredox Catalysis: The Activation of Aryl Bromides. *Chem.—Eur. J.* **2015**, *21*, 15496−15501.

(22) Häring, M.; Pérez-Ruiz, R.; Jacobi von Wangelin, A.; Díaz, D. D. Intragel photoreduction of aryl halides by green-to-blue upconversion under aerobic conditions. *Chem. Commun.* **2015**, *51*, 16848−16851.

(23) Khnayzer, R. S.; Blumhoff, J.; Harrington, J. A.; Haefele, A.; Deng, F.; Castellano, F. N. Upconversion-powered photoelectrochemistry. *Chem. Commun.* **2012**, *48*, 209−211.

(24) Zeng, L.; Huang, L.; Lin, W.; Jiang, L.-H.; Han, G. Red light-driven electron sacrificial agents-free photoreduction of inert aryl halides via triplet-triplet annihilation. *Nat. Commun.* **2023**, *14*, 1102.

(25) Liang, W.; Nie, C.; Du, J.; Han, Y.; Zhao, G.; Yang, F.; Liang, G.; Wu, K. Near-infrared photon upconversion and solar synthesis using lead-free nanocrystals. *Nat. Photon.* **2023**, *17*, 346−353.

(26) Tokunaga, A.; Uriarte, L. M.; Mutoh, K.; Fron, E.; Hofkens, J.; Sliwa, M.; Abe, J. Photochromic Reaction by Red Light via Triplet Fusion Upconversion. *J. Am. Chem. Soc.* **2019**, *141*, 17744−17753.

(27) Kerzig, C.; Wenger, O. S. Sensitized triplet−triplet annihilation upconversion in water and its application to photochemical transformations. *Chem. Sci.* **2018**, *9*, 6670−6678.

(28) Wang, C.; Reichenauer, F.; Kitzmann, W. R.; Kerzig, C.; Heinze, K.; Resch-Genger, U. Efficient Triplet-Triplet Annihilation Upconversion Sensitized by a Chromium(III) Complex via an Underexplored Energy Transfer Mechanism. *Angew. Chem., Int. Ed.* **2022**, *61*, No. e202202238.

(29) Islangulov, R. R.; Castellano, F. N. Photochemical upconversion: Anthracene dimerization sensitized to visible light by a Ru^{II} chromophore. *Angew. Chem., Int. Ed.* **2006**, *45*, 5957−5959.

(30) Harada, N.; Sasaki, Y.; Hosoyamada, M.; Kimizuka, N.; Yanai, N. Discovery of Key TIPS-Naphthalene for Efficient Visible-to-UV Photon Upconversion under Sunlight and Room Light. *Angew. Chem., Int. Ed.* **2021**, *60*, 142−147.

(31) VanOrman, Z. A.; Nienhaus, L. Feeling blue no more: How TIPS-naphthalene enables efficient visible-to-UV upconversion. *Matter* **2021**, *4*, 2625−2626.

(32) Murakami, Y.; Motooka, A.; Enomoto, R.; Niimi, K.; Kaiho, A.; Kiyoyanagi, N. Visible-to-ultraviolet (<340 nm) photon upconversion by triplet−triplet annihilation in solvents. *Phys. Chem. Chem. Phys.* **2020**, *22*, 27134−27143.

(33) Zhao, W.; Castellano, F. N. Upconverted Emission from Pyrene and Di-*tert*-butylpyrene Using $Ir(ppy)_3$ as Triplet Sensitizer. *J. Phys. Chem. A* **2006**, *110*, 11440−11445.

(34) Singh-Rachford, T. N.; Castellano, F. N. Low Power Visible-to-UV Upconversion. *J. Phys. Chem. A* **2009**, *113*, 5912−5917.

(35) Duan, P.; Yanai, N.; Kimizuka, N. A bis-cyclometalated iridium complex as a benchmark sensitizer for efficient visible-to-UV photon upconversion. *Chem. Commun.* **2014**, *50*, 13111−13113.

(36) Yanai, N.; Kozue, M.; Amemori, S.; Kabe, R.; Adachi, C.; Kimizuka, N. Increased vis-to-UV upconversion performance by energy level matching between a TADF donor and high triplet energy acceptors. *J. Mater. Chem. C* **2016**, *4*, 6447−6451.

(37) Gray, V.; Xia, P.; Huang, Z.; Moses, E.; Fast, A.; Fishman, D. A.; Vullev, V. I.; Abrahamsson, M.; Moth-Poulsen, K.; Lee Tang, M. CdS/ZnS core−shell nanocrystal photosensitizers for visible to UV upconversion. *Chem. Sci.* **2017**, *8*, 5488−5496.

(38) Hisamitsu, S.; Miyano, J.; Okumura, K.; Ka-Ho Hui, J.; Yanai, N.; Kimizuka, N. Visible-to-UV Photon Upconversion in Nanostructured Chromophoric Ionic Liquids. *ChemistryOpen* **2020**, *9*, 3−17.

(39) Merkel, P. B.; Dinnocenzo, J. P. Low-power green-to-blue and blue-to-UV upconversion in rigid polymer films. *J. Lumin.* **2009**, *129*, 303−306.

(40) Lin, X.; Chen, Z.; Han, Y.; Nie, C.; Xia, P.; He, S.; Li, J.; Wu, K. ZnSe/ZnS Core/Shell Quantum Dots as Triplet Sensitizers toward

https://doi.org/10.1021/jacs.3c02609
J. Am. Chem. Soc. 2023, 145, 11402−11414

Visible-to-Ultraviolet B Photon Upconversion. *ACS Energy Lett.* **2022**, *7*, 914−919.
(41) He, S.; Luo, X.; Liu, X.; Li, Y.; Wu, K. Visible-to-Ultraviolet Upconversion Efficiency above 10% Sensitized by Quantum-Confined Perovskite Nanocrystals. *J. Phys. Chem. Lett.* **2019**, *10*, 5036−5040.
(42) Hou, L.; Olesund, A.; Thurakkal, S.; Zhang, X.; Albinsson, B. Efficient Visible-to-UV Photon Upconversion Systems Based on CdS Nanocrystals Modified with Triplet Energy Mediators. *Adv. Funct. Mater.* **2021**, *31*, 2106198.
(43) Chen, Q.; Liu, Y.; Guo, X.; Peng, J.; Garakyaraghi, S.; Papa, C. M.; Castellano, F. N.; Zhao, D.; Ma, Y. Energy Transfer Dynamics in Triplet−Triplet Annihilation Upconversion Using a Bichromophoric Heavy-Atom-Free Sensitizer. *J. Phys. Chem. A* **2018**, *122*, 6673−6682.
(44) Kübler, J. A.; Pfund, B.; Wenger, O. S. Zinc(II) Complexes with Triplet Charge-Transfer Excited States Enabling Energy-Transfer Catalysis, Photoinduced Electron Transfer, and Upconversion. *JACS Au* **2022**, *2*, 2367−2380.
(45) Du, Y.; Ai, X.; Li, Z.; Sun, T.; Huang, Y.; Zeng, X.; Chen, X.; Rao, F.; Wang, F. Visible-to-Ultraviolet Light Conversion: Materials and Applications. *Adv. Photonics Res.* **2021**, *2*, 2000213.
(46) Schmid, L.; Glaser, F.; Schaer, R.; Wenger, O. S. High Triplet Energy Iridium(III) Isocyanoborato Complex for Photochemical Upconversion, Photoredox and Energy Transfer Catalysis. *J. Am. Chem. Soc.* **2022**, *144*, 963−976.
(47) Uji, M.; Zähringer, T. J. B.; Kerzig, C.; Yanai, N. Visible-to-UV Photon Upconversion: Recent Progress in New Materials and Applications. *Angew. Chem., Int. Ed.* **2023**, No. e202301506.
(48) Zähringer, T. J. B.; Bertrams, M.-S.; Kerzig, C. Purely organic Vis-to-UV upconversion with an excited annihilator singlet beyond 4 eV. *J. Mater. Chem. C* **2022**, *10*, 4568−4573.
(49) Pfund, B.; Steffen, D. M.; Schreier, M. R.; Bertrams, M.-S.; Ye, C.; Börjesson, K.; Wenger, O. S.; Kerzig, C. UV Light Generation and Challenging Photoreactions Enabled by Upconversion in Water. *J. Am. Chem. Soc.* **2020**, *142*, 10468−10476.
(50) Awwad, N.; Bui, A. T.; Danilov, E. O.; Castellano, F. N. Visible-Light-Initiated Free-Radical Polymerization by Homomolecular Triplet-Triplet Annihilation. *Chem* **2020**, *6*, 3071−3085.
(51) Barawi, M.; Fresno, F.; Pérez-Ruiz, R.; de la Peña O'Shea, V. A. Photoelectrochemical Hydrogen Evolution Driven by Visible-to-Ultraviolet Photon Upconversion. *ACS Appl. Energy Mater.* **2019**, *2*, 207−211.
(52) Ravetz, B. D.; Tay, N. E. S.; Joe, C. L.; Sezen-Edmonds, M.; Schmidt, M. A.; Tan, Y.; Janey, J. M.; Eastgate, M. D.; Rovis, T. Development of a Platform for Near-Infrared Photoredox Catalysis. *ACS Cent. Sci.* **2020**, *6*, 2053−2059.
(53) Wei, Y.; Pan, K.; Cao, X.; Li, Y.; Zhou, X.; Yang, C. Multiple Resonance Thermally Activated Delayed Fluorescence Sensitizers Enable Green-to-Ultraviolet Photon Upconversion: Application in Photochemical Transformations. *CCS Chem.* **2022**, *4*, 3852−3863.
(54) Zähringer, T. J. B.; Moghtader, J. A.; Bertrams, M.-S.; Roy, B.; Uji, M.; Yanai, N.; Kerzig, C. Blue-to-UVB Upconversion, Solvent Sensitization and Challenging Bond Activation Enabled by a Benzene-Based Annihilator. *Angew. Chem., Int. Ed.* **2023**, *62*, No. e202215340.
(55) Zhou, Y.; Castellano, F. N.; Schmidt, T. W.; Hanson, K. On the Quantum Yield of Photon Upconversion via Triplet−Triplet Annihilation. *ACS Energy Lett.* **2020**, *5*, 2322−2326.
(56) Kalpattu, A.; Dilbeck, T.; Hanson, K.; Fourkas, J. T. Extracting accurate information from triplet−triplet annihilation upconversion data with a mass-conserving kinetic model. *Phys. Chem. Chem. Phys.* **2022**, *24*, 28174−28190.
(57) Rowe, J. M.; Zhu, J.; Soderstrom, E. M.; Xu, W.; Yakovenko, A.; Morris, A. J. Sensitized photon upconversion in anthracene-based zirconium metal−organic frameworks. *Chem. Commun.* **2018**, *54*, 7798−7801.
(58) Yang, M.; Sheykhi, S.; Zhang, Y.; Milsmann, C.; Castellano, F. N. Low power threshold photochemical upconversion using a zirconium(IV) LMCT photosensitizer. *Chem. Sci.* **2021**, *12*, 9069−9077.
(59) McClenaghan, N. D.; Leydet, Y.; Maubert, B.; Indelli, M. T.; Campagna, S. Excited-state equilibration: a process leading to long-lived metal-to-ligand charge transfer luminescence in supramolecular systems. *Coord. Chem. Rev.* **2005**, *249*, 1336−1350.
(60) Baba, A. I.; Shaw, J. R.; Simon, J. A.; Thummel, R. P.; Schmehl, R. H. The photophysical behavior of d^6 complexes having nearly isoenergetic MLCT and ligand localized excited states. *Coord. Chem. Rev.* **1998**, *171*, 43−59.
(61) Lavie-Cambot, A.; Lincheneau, C.; Cantuel, M.; Leydet, Y.; McClenaghan, N. D. Reversible electronic energy transfer: a means to govern excited-state properties of supramolecular systems. *Chem. Soc. Rev.* **2010**, *39*, 506−515.
(62) Kazama, A.; Imai, Y.; Okayasu, Y.; Yamada, Y.; Yuasa, J.; Aoki, S. Design and Synthesis of Cyclometalated Iridium(III) Complexes—Chromophore Hybrids that Exhibit Long-Emission Lifetimes Based on a Reversible Electronic Energy Transfer Mechanism. *Inorg. Chem.* **2020**, *59*, 6905−6922.
(63) Sasaki, Y.; Yanai, N.; Kimizuka, N. Osmium Complex−Chromophore Conjugates with Both Singlet-to-Triplet Absorption and Long Triplet Lifetime through Tuning of the Heavy-Atom Effect. *Inorg. Chem.* **2022**, *61*, 5982−5990.
(64) Kozlov, D. V.; Castellano, F. N. Anti-Stokes delayed fluorescence from metal−organic bichromophores. *Chem. Commun.* **2004**, 2860−2861.
(65) Lu, Y.; Wang, J.; McGoldrick, N.; Cui, X.; Zhao, J.; Caverly, C.; Twamley, B.; Ó Máille, G. M.; Irwin, B.; Conway-Kenny, R.; Draper, S. M. Iridium(III) Complexes Bearing Pyrene-Functionalized 1,10-Phenanthroline Ligands as Highly Efficient Sensitizers for Triplet−Triplet Annihilation Upconversion. *Angew. Chem., Int. Ed.* **2016**, *55*, 14688−14692.
(66) Lu, Y.; Conway-Kenny, R.; Wang, J.; Cui, X.; Zhao, J.; Draper, S. M. Exploiting coumarin-6 as ancillary ligands in 1,10-phenanthroline Ir(III) complexes: generating triplet photosensitisers with high upconversion capabilities. *Dalton Trans.* **2018**, *47*, 8585−8589.
(67) Ji, S.; Wu, W.; Wu, W.; Guo, H.; Zhao, J. Ruthenium(II) Polyimine Complexes with a Long-Lived ^{3}IL Excited State or a ^{3}MLCT/^{3}IL Equilibrium: Efficient Triplet Sensitizers for Low-Power Upconversion. *Angew. Chem., Int. Ed.* **2011**, *50*, 1626−1629.
(68) Howarth, A. J.; Majewski, M. B.; Wolf, M. O. Photophysical properties and applications of coordination complexes incorporating pyrene. *Coord. Chem. Rev.* **2015**, *282*−*283*, 139−149.
(69) Simon, J. A.; Curry, S. L.; Schmehl, R. H.; Schatz, T. R.; Piotrowiak, P.; Jin, X. Q.; Thummel, R. P. Intramolecular electronic energy transfer in ruthenium(II) diimine donor pyrene acceptor complexes linked by a single C-C bond. *J. Am. Chem. Soc.* **1997**, *119*, 11012−11022.
(70) Gu, J.; Chen, J.; Schmehl, R. H. Using Intramolecular Energy Transfer to Transform non-Photoactive, Visible-Light-Absorbing Chromophores into Sensitizers for Photoredox Reactions. *J. Am. Chem. Soc.* **2010**, *132*, 7338−7346.
(71) Strieth-Kalthoff, F.; Glorius, F. Triplet Energy Transfer Photocatalysis: Unlocking the Next Level. *Chem* **2020**, *6*, 1888−1903.
(72) Mills, I. N.; Porras, J. A.; Bernhard, S. Judicious Design of Cationic, Cyclometalated Ir^{III} Complexes for Photochemical Energy Conversion and Optoelectronics. *Acc. Chem. Res.* **2018**, *51*, 352−364.
(73) Peng, J.; Jiang, X.; Guo, X.; Zhao, D.; Ma, Y. Sensitizer design for efficient triplet−triplet annihilation upconversion: annihilator-appended tris-cyclometalated Ir(III) complexes. *Chem. Commun.* **2014**, *50*, 7828−7830.
(74) Denisov, S. A.; Cudré, Y.; Verwilst, P.; Jonusauskas, G.; Marín-Suárez, M.; Fernández-Sánchez, J. F.; Baranoff, E.; McClenaghan, N. D. Direct Observation of Reversible Electronic Energy Transfer Involving an Iridium Center. *Inorg. Chem.* **2014**, *53*, 2677−2682.
(75) Davidson, R.; Hsu, Y.-T.; Fox, M. A.; Aguilar, J. A.; Yufit, D.; Beeby, A. Tuning Emission Lifetimes of $Ir(C^N)_2(acac)$ Complexes with Oligo(phenyleneethynylene) Groups. *Inorg. Chem.* **2023**, *62*, 2793−2805.
(76) Thompson, M. P.; Agger, J.; Wong, L. S. Paternò−Büchi Reaction as a Demonstration of Chemical Kinetics and Synthetic

Photochemistry Using a Light Emitting Diode Apparatus. *J. Chem. Educ.* **2015**, *92*, 1716−1720.
(77) Soika, J.; McLaughlin, C.; Neveselý, T.; Daniliuc, C. G.; Molloy, J. J.; Gilmour, R. Organophotocatalytic N−O Bond Cleavage of Weinreb Amides: Mechanism-Guided Evolution of a PET to ConPET Platform. *ACS Catal.* **2022**, *12*, 10047−10056.
(78) Montalti, M.; Credi, A.; Prodi, L.; Gandolfi, M. T. *Handbook of Photochemistry*; CRC Taylor & Francis: Boca Raton, Florida, 2006.
(79) DiLuzio, S.; Connell, T. U.; Mdluli, V.; Kowalewski, J. F.; Bernhard, S. Understanding Ir(III) Photocatalyst Structure−Activity Relationships: A Highly Parallelized Study of Light-Driven Metal Reduction Processes. *J. Am. Chem. Soc.* **2022**, *144*, 1431−1444.
(80) Bevernaegie, R.; Wehlin, S. A. M.; Elias, B.; Troian-Gautier, L. A Roadmap Towards Visible Light Mediated Electron Transfer Chemistry with Iridium(III) Complexes. *ChemPhotoChem* **2021**, *5*, 185−234.
(81) Porter, G.; Wilkinson, F. Energy transfer from the triplet state. *Proc. R. Soc. London, Ser. A* **1961**, *264*, 1−18.
(82) Chen, K.; Hussain, M.; Razi, S. S.; Hou, Y.; Yildiz, E. A.; Zhao, J.; Yaglioglu, H. G.; Donato, M. D. Anthryl-Appended Platinum(II) Schiff Base Complexes: Exceptionally Small Stokes Shift, Triplet Excited States Equilibrium, and Application in Triplet−Triplet-Annihilation Upconversion. *Inorg. Chem.* **2020**, *59*, 14731−14745.
(83) Schmid, M.-A.; Brückmann, J.; Bösking, J.; Nauroozi, D.; Karnahl, M.; Rau, S.; Tschierlei, S. Merging of a Perylene Moiety Enables a Ru^{II} Photosensitizer with Long-Lived Excited States and the Efficient Production of Singlet Oxygen. *Chem.—Eur. J.* **2022**, *28*, No. e202103609.
(84) Indelli, M. T.; Ghirotti, M.; Prodi, A.; Chiorboli, C.; Scandola, F.; McClenaghan, N. D.; Puntoriero, F.; Campagna, S. Solvent Switching of Intramolecular Energy Transfer in Bichromophoric Systems: Photophysics of (2,2′-Bipyridine)tetracyanoruthenate(II)/Pyrenyl Complexes. *Inorg. Chem.* **2003**, *42*, 5489−5497.
(85) Merkel, P. B.; Dinnocenzo, J. P. Thermodynamic energies of donor and acceptor triplet states. *J. Photochem. Photobiol., A* **2008**, *193*, 110−121.
(86) Johnston, L. J.; Kanigan, T. Electron transfer reactions between bis(4-methoxophenyl)methyl cations and triplet 1-methoxynaphthalene. *J. Am. Chem. Soc.* **1990**, *112*, 1271−1273.
(87) Sakamoto, M.; Cai, X.; Hara, M.; Fujitsuka, M.; Majima, T. Intermolecular Electron Transfer from Naphthalene Derivatives in the Higher Triplet Excited States. *J. Am. Chem. Soc.* **2004**, *126*, 9709−9714.
(88) Cai, X.; Sakamoto, M.; Hara, M.; Tojo, S.; Kawai, K.; Endo, M.; Fujitsuka, M.; Majima, T. Transient Phenomena of Polyphenyls in the Higher Triplet Excited State. *J. Phys. Chem. A* **2004**, *108*, 9361−9364.
(89) Kocia, R. Pulse radiolysis studies of intermediates derived from *p*-terphenyl in the oxygenated methyltributylammonium bis-[(trifluoromethyl)sulfonyl]imide ionic liquid. *Int. J. Chem. Kinet.* **2019**, *51*, 958−964.
(90) Monguzzi, A.; Mezyk, J.; Scotognella, F.; Tubino, R.; Meinardi, F. Upconversion-induced fluorescence in multicomponent systems: Steady-state excitation power threshold. *Phys. Rev. B* **2008**, *78*, 195112.
(91) Durandin, N. A.; Isokuortti, J.; Efimov, A.; Vuorimaa-Laukkanen, E.; Tkachenko, N. V.; Laaksonen, T. Critical Sensitizer Quality Attributes for Efficient Triplet−Triplet Annihilation Upconversion with Low Power Density Thresholds. *J. Phys. Chem. C* **2019**, *123*, 22865−22872.
(92) Olesund, A.; Johnsson, J.; Edhborg, F.; Ghasemi, S.; Moth-Poulsen, K.; Albinsson, B. Approaching the Spin-Statistical Limit in Visible-to-Ultraviolet Photon Upconversion. *J. Am. Chem. Soc.* **2022**, *144*, 3706−3716.
(93) Edhborg, F.; Olesund, A.; Albinsson, B. Best practice in determining key photophysical parameters in triplet−triplet annihilation photon upconversion. *Photochem. Photobiol. Sci.* **2022**, *21*, 1143−1158.
(94) Monguzzi, A.; Tubino, R.; Hoseinkhani, S.; Campione, M.; Meinardi, F. Low power, non-coherent sensitized photon up-conversion: modelling and perspectives. *Phys. Chem. Chem. Phys.* **2012**, *14*, 4322−4332.
(95) Ronchi, A.; Monguzzi, A. Sensitized triplet−triplet annihilation based photon upconversion in full organic and hybrid multicomponent systems. *Chem. Phys. Rev.* **2022**, *3*, 041301.
(96) Carrod, A. J.; Gray, V.; Börjesson, K. Recent advances in triplet−triplet annihilation upconversion and singlet fission, towards solar energy applications. *Energy Environ. Sci.* **2022**, *15*, 4982−5016.
(97) Gholizadeh, E. M.; Prasad, S. K. K.; Teh, Z. L.; Ishwara, T.; Norman, S.; Petty, A. J.; Cole, J. H.; Cheong, S.; Tilley, R. D.; Anthony, J. E.; Huang, S.; Schmidt, T. W. Photochemical upconversion of near-infrared light from below the silicon bandgap. *Nat. Photon.* **2020**, *14*, 585−590.
(98) Olesund, A.; Gray, V.; Mårtensson, J.; Albinsson, B. Diphenylanthracene Dimers for Triplet−Triplet Annihilation Photon Upconversion: Mechanistic Insights for Intramolecular Pathways and the Importance of Molecular Geometry. *J. Am. Chem. Soc.* **2021**, *143*, 5745−5754.
(99) Imperiale, C. J.; Green, P. B.; Hasham, M.; Wilson, M. W. B. Ultra-small PbS nanocrystals as sensitizers for red-to-blue triplet-fusion upconversion. *Chem. Sci.* **2021**, *12*, 14111−14120.
(100) Meroni, D.; Monguzzi, A.; Meinardi, F. Photon upconversion in multicomponent systems: Role of back energy transfer. *J. Chem. Phys.* **2020**, *153*, 114302.
(101) Perego, J.; Pedrini, J.; Bezuidenhout, C. X.; Sozzani, P. E.; Meinardi, F.; Bracco, S.; Comotti, A.; Monguzzi, A. Engineering Porous Emitting Framework Nanoparticles with Integrated Sensitizers for Low-Power Photon Upconversion by Triplet Fusion. *Adv. Mater.* **2019**, *31*, 1903309.
(102) Schmid, L.; Kerzig, C.; Prescimone, A.; Wenger, O. S. Photostable Ruthenium(II) Isocyanoborato Luminophores and Their Use in Energy Transfer and Photoredox Catalysis. *JACS Au* **2021**, *1*, 819−832.
(103) Mateos, J.; Rigodanza, F.; Vega-Peñaloza, A.; Sartorel, A.; Natali, M.; Bortolato, T.; Pelosi, G.; Companyó, X.; Bonchio, M.; Dell'Amico, L. Naphthochromenones: Organic Bimodal Photocatalysts Engaging in Both Oxidative and Reductive Quenching Processes. *Angew. Chem., Int. Ed.* **2020**, *59*, 1302−1312.
(104) Kim, D.; Teets, T. S. Strategies for accessing photosensitizers with extreme redox potentials. *Chem. Phys. Rev.* **2022**, *3*, 021302.
(105) Griesbeck, A. G.; Buhr, S.; Fiege, M.; Schmickler, H.; Lex, J. Stereoselectivity of Triplet Photocycloadditions:1 Diene−Carbonyl Reactions and Solvent Effects. *J. Org. Chem.* **1998**, *63*, 3847−3854.
(106) Castellanos-Soriano, J.; Álvarez-Gutiérrez, D.; Jiménez, M. C.; Pérez-Ruiz, R. Photoredox catalysis powered by triplet fusion upconversion: arylation of heteroarenes. *Photochem. Photobiol. Sci.* **2022**, *21*, 1175−1184.
(107) Liu, S.; Liu, H.; Shen, L.; Xiao, Z.; Hu, Y.; Zhou, J.; Wang, X.; Liu, Z.; Li, Z.; Li, X. Applying triplet-triplet annihilation upconversion in degradation of oxidized lignin model with good selectivity. *Chem. Eng. J.* **2022**, *431*, 133377.
(108) Freitag, M.; Möller, N.; Rühling, A.; Strassert, C. A.; Ravoo, B. J.; Glorius, F. Photocatalysis in the Dark: Near-Infrared Light Driven Photoredox Catalysis by an Upconversion Nanoparticle/Photocatalyst System. *ChemPhotoChem* **2019**, *3*, 24−27.
(109) Bilger, J. B.; Kerzig, C.; Larsen, C. B.; Wenger, O. S. A Photorobust Mo(0) Complex Mimicking $[Os(2,2'\text{-bipyridine})_3]^{2+}$ and Its Application in Red-to-Blue Upconversion. *J. Am. Chem. Soc.* **2021**, *143*, 1651−1663.
(110) Börjesson, K.; Dzebo, D.; Albinsson, B.; Moth-Poulsen, K. Photon upconversion facilitated molecular solar energy storage. *J. Mater. Chem. A* **2013**, *1*, 8521−8524.
(111) Michalska, W. Z.; Halcovitch, N. R.; Coote, S. C. Synthesis of functionalized spirocyclic oxetanes through Paternò−Büchi reactions of cyclic ketones and maleic acid derivatives. *Chem. Commun.* **2023**, *59*, 784−787.
(112) Franceschi, P.; Cuadros, S.; Goti, G.; Dell'Amico, L. Mechanisms and Synthetic Strategies in Visible Light-Driven [2+2]-

https://doi.org/10.1021/jacs.3c02609
J. Am. Chem. Soc. 2023, 145, 11402−11414

Heterocycloadditions. *Angew. Chem., Int. Ed.* **2023**, *62*, No. e202217210.
(113) Rykaczewski, K. A.; Schindler, C. S. Visible-Light-Enabled Paternò−Büchi Reaction via Triplet Energy Transfer for the Synthesis of Oxetanes. *Org. Lett.* **2020**, *22*, 6516−6519.
(114) Becker, M. R.; Richardson, A. D.; Schindler, C. S. Functionalized azetidines via visible light-enabled aza Paternò-Büchi reactions. *Nat. Commun.* **2019**, *10*, 5095.
(115) Liu, Y.; Ni, D.; Stevenson, B. G.; Tripathy, V.; Braley, S. E.; Raghavachari, K.; Swierk, J. R.; Brown, M. K. Photosensitized [2+2]-Cycloadditions of Alkenylboronates and Alkenes. *Angew. Chem., Int. Ed.* **2022**, *61*, No. e202200725.
(116) Mateos, J.; Rigodanza, F.; Costa, P.; Natali, M.; Vega-Peñaloza, A.; Fresch, E.; Collini, E.; Bonchio, M.; Sartorel, A.; Dell'Amico, L. Unveiling the impact of the light source and steric factors on [2+2] heterocycloaddition reactions. *Nat. Synth.* **2022**, *2*, 26−36.
(117) Wegeberg, C.; Häussinger, D.; Wenger, O. S. Pyrene-Decoration of a Chromium(0) Tris(diisocyanide) Enhances Excited State Delocalization: A Strategy to Improve the Photoluminescence of $3d^6$ Metal Complexes. *J. Am. Chem. Soc.* **2021**, *143*, 15800−15811.
(118) Liu, S.; Wang, X.; Liu, H.; Shen, L.; Zhao, D.; Li, X. Enhancing triplet sensitization ability of donor−acceptor dyads via intramolecular triplet energy transfer. *J. Mater. Chem. C* **2020**, *8*, 3536−3544.
(119) Wu, W.; Sun, J.; Ji, S.; Wu, W.; Zhao, J.; Guo, H. Tuning the emissive triplet excited states of platinum(II) Schiff base complexes with pyrene, and application for luminescent oxygen sensing and triplet−triplet-annihilation based upconversions. *Dalton Trans.* **2011**, *40*, 11550−11561.
(120) Schreier, M. R.; Guo, X.; Pfund, B.; Okamoto, Y.; Ward, T. R.; Kerzig, C.; Wenger, O. S. Water-Soluble Tris(cyclometalated) Iridium(III) Complexes for Aqueous Electron and Energy Transfer Photochemistry. *Acc. Chem. Res.* **2022**, *55*, 1290−1300.
(121) Poplata, S.; Tröster, A.; Zou, Y.-Q.; Bach, T. Recent Advances in the Synthesis of Cyclobutanes by Olefin [2 + 2] Photocycloaddition Reactions. *Chem. Rev.* **2016**, *116*, 9748−9815.
(122) Paulisch, T. O.; Mai, L. A.; Strieth-Kalthoff, F.; James, M. J.; Henkel, C.; Guldi, D. M.; Glorius, F. Dynamic Kinetic Sensitization of *β*-Dicarbonyl Compounds—Access to Medium-Sized Rings by De Mayo-Type Ring Expansion. *Angew. Chem., Int. Ed.* **2022**, *61*, No. e202112695.

https://doi.org/10.1021/jacs.3c02609
J. Am. Chem. Soc. 2023, 145, 11402−11414